

PAPER

The use of low duty cycle pulsed-unipolar current mode for producing Alumina/ZnO nanocomposite coatings via plasma electrolytic oxidation process

To cite this article: Safoora Shahzamani *et al* 2019 *Mater. Res. Express* **6** 076555

View the [article online](#) for updates and enhancements.



IOP | ebooks™



Bringing together innovative digital publishing with leading authors from the global scientific community.

Start exploring the collection—download the first chapter of every title for free.



PAPER

The use of low duty cycle pulsed-unipolar current mode for producing Alumina/ZnO nanocomposite coatings via plasma electrolytic oxidation process

RECEIVED
3 March 2019REVISED
24 March 2019ACCEPTED FOR PUBLICATION
5 April 2019PUBLISHED
17 April 2019Safoora Shahzamani¹ , Ali Ashrafi^{1,3} , Mohammad Reza Toroghinejad¹, Vahid Dehnavi² and Amin Hakimizad¹¹ Department of Materials Engineering, Isfahan University of Technology, Isfahan 84156-83111, Iran² Department of Chemistry, The University of Western Ontario, London, ON, N6A 5B7, Canada³ Author to whom any correspondence should be addressed.E-mail: safoora.shahzamani@ma.iut.ac.ir and ashrafi@cc.iut.ac.ir

Keywords: aluminum, plasma electrolytic oxidation, composite coating, alumina, ZnO

Abstract

The incorporation of ZnO nanoparticles into plasma electrolytic oxidation coatings formed on aluminum was investigated in this work. The coating process was performed in silicate-based electrolytes containing varying amounts of ZnO nanoparticles. A current density of 5 A dm^{-2} with a low duty cycle of 20% and a frequency of 2000 Hz were applied to all aluminum samples. Results showed all coatings were primarily comprised of $\gamma\text{-Al}_2\text{O}_3$, $\text{Al}_2\text{H}_2\text{O}_{12}\text{S}_4$ ($\text{Al}_2\text{O}_3 \cdot 4\text{SiO}_2 \cdot \text{H}_2\text{O}$) and contained ZnO nanoparticles from the electrolyte. Surface and cross-sectional elemental maps revealed that ZnO nanoparticles were distributed primarily on the coating surface and near the coating-substrate interface. It has been proposed that formation of silica insoluble gel containing entrapped ZnO nanoparticles on the coating surface is a reason of why Zn and Si were primarily concentrated in the upper parts of the coatings. Beside this, particles can only reach the inner layer of the coating through short-circuit paths formed by breakdown events. In pulsed-unipolar DC current mode with low duty cycle and corresponding large number of micro-discharges, higher number of nanoparticles can enter discharge channels and reach the inner parts of the coating. Potentiodynamic polarization test results showed embedding nanoparticles in the coating structure improves its corrosion behavior.

1. Introduction

Plasma electrolytic oxidation (PEO), also known as micro-arc oxidation (MAO), is a relatively novel technique to produce oxide ceramic coatings [1]. The process is typically performed on lightweight valve metals including Al [2–5], Ti [6], Mg [7], as well as their alloys [5]. PEO results in the formation of relatively thick, ceramic-like coatings containing amorphous and crystalline phases [1–3]. PEO is similar to a conventional anodizing process in principle; however, the applied potentials should be sufficiently high to exceed the dielectric breakdown field at flaws in the coating as it grows [4]. The process often involves simultaneous local melting of the coating and rapid quenching of the solidified products [1]. In this regard, mechanisms such as anodic oxidation, thermal oxidation and plasma chemical reactions may participate in the formation of the coating [3]. Application of PEO coatings improves the surface performance, resulting in higher hardness, better wear protection and improved corrosion resistance [2]. In addition, PEO is a cost-effective and environmentally friendly process [5].

Species in the PEO coating originate from both the substrate and the electrolyte. It is possible to form composite coatings during the PEO process by adding insoluble particles to the electrolyte. Previous research studies have shown that metal oxide nanoparticles like ZnO [5], ZrO_2 [7, 8], TiO_2 [9, 10] and Al_2O_3 [11] are good candidates to be used as the second phase in PEO composite coatings. Particles in electrolyte suspensions are usually incorporated into the outer parts of coatings. They can reach the inner layers via short-circuit paths [7] or

Table 1. The chemical composition of aluminum substrates.

Element	Fe	Si	Mg	Cu	Ti	Zn	Mn	Al
Content (wt%)	0.4	0.25	0.005	0.05	0.03	0.05	0.05	Balance

as a result of the cataphoretic effect which makes it possible to transfer particles both to and away from the substrate in the strong electric fields during PEO [11, 12]. Embedding nanoparticles in the coating structure improves its corrosion behavior and tribological properties and increases its hardness and adhesion to the substrate [9–11]. A series of prior studies have explored the influence of electrolyte additives on PEO coating properties. Results showed that adding Na_2WO_4 promoted the formation of high impedance coatings and decreased the breakdown voltage and energy consumption. Furthermore, it has been shown to increase the coating thickness, density and corrosion resistance [12, 13].

Research on alumina-based ceramic nanocomposites during the past decade was mainly focused on the addition of one or several reinforcement phases such as metal oxide nanoparticles [14]. Zinc oxide (ZnO) is an excellent choice as a reinforcement for alumina-based composites. It has a high thermal, chemical and mechanical stability in addition to its thermodynamic compatibility with Al_2O_3 [14].

Stojadinovic *et al* reported the formation of $\text{Al}_2\text{O}_3/\text{ZnO}$ oxide coatings by conventional DC PEO on aluminum [5]. They used water-based boric acid and borax electrolyte with the addition of ZnO nanoparticles. They were not able to detect any peaks corresponding to ZnO in the XRD patterns after different PEO treatment durations, most probably due to the low concentration of ZnO nanoparticles in the coating. To investigate the presence of ZnO nanoparticles in oxide coatings, they performed Raman measurements and EDS analysis. Results showed that the concentration of Zn (originating from ZnO nanoparticles) was less in the inner layer compared with the outer layer.

The present work investigates the incorporation of ZnO nanoparticles into coatings formed on aluminum by PEO. The main objective of the present study was to obtain an alumina–zinc oxide nanocomposite coating and to describe coating microstructures. For this purpose, a pulsed-unipolar current with a low duty cycle was chosen and nanoparticles embedded in the upper parts of the coating and in the inner regions especially near to the coating-substrate interface. Nanocomposite oxide coatings may be of interest for various applications such as electrodes for optoelectronic devices. They can be used as photovoltaic solar cells, liquid crystal displays or light emitting diodes [14, 15]. In addition, probable reactions occurring during each period of the process in the presence of ZnO nanoparticles have been discussed.

2. Materials and methods

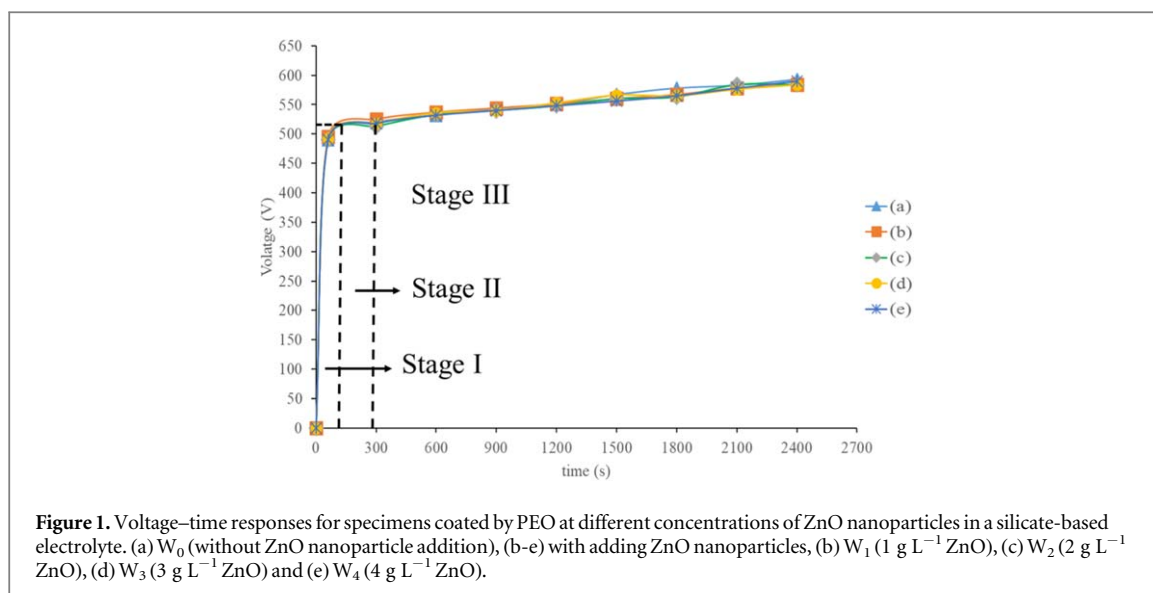
The chemical composition of 1050 aluminum used as the substrate is presented in table 1. Specimens with dimensions of 1 mm × 25 mm × 100 mm were degreased and cleaned ultrasonically in acetone and ethanol, rinsed in deionized water, and finally dried in warm air.

The PEO process was carried out in a silicate-based electrolyte containing 10 g L⁻¹ Na_2SiO_3 , 2 g L⁻¹ KOH and 2 g L⁻¹ Na_2WO_4 . ZnO nanoparticles with a particle size in the range of 150–300 nm were added as required. Samples were labelled as W_0 – W_4 . The subscripts represent the content of ZnO nanoparticles in the PEO electrolytes for 0, 1, 2, 3 and 4 g L⁻¹ respectively.

The zeta potential is a crucial factor in determining the stability of a colloidal dispersion. A suspension of particles with a high absolute value of zeta potential is more stable and resists agglomeration and settling more compared with suspensions with lower absolute values of zeta potential. The zeta potential can be varied by adjusting the pH. Increasing the pH level generally shifts zeta potential towards more negative values [16]. Therefore, it is necessary to adjust the pH of the electrolyte at a suitable level in order to have a stable ZnO suspension [17, 18]. Alkaline electrolytes containing potassium hydroxide and sodium silicate with pH values larger than 12 are most commonly used in PEO [4, 11, 19]. The silicate-based electrolyte used in this research had a pH of approximately 12. At this pH, ZnO nanoparticles have a high, negative zeta potential and are stable in the electrolyte. A high absolute value of zeta potential is desirable in PEO electrolytes containing particles since it will enhance particle movement under a given electric field and promotes the incorporation of particles into the coating.

PEO treatment was carried out under pulsed-unipolar DC mode using a built in-house rectifier with a maximum output of 700 V/30 A. Samples were treated at a constant current density of 5 A dm⁻², a duty cycle of 20%, and a frequency of 2000 Hz for 40 min. The duty cycle is defined as:

$$D_t = [t_{\text{on}} / (t_{\text{on}} + t_{\text{off}})] \times 100$$



where t_{on} is the ‘on’ period and t_{off} is the ‘off’ period during a single cycle [19]. During the coating process, the electrolyte was continuously stirred with a centrifugal pump and its temperature was maintained at $\sim 293 \text{ K}$. Two 316 L stainless steel sheets ($10 \text{ cm} \times 15 \text{ cm}$) were used as the cathode. Samples were coated under galvanostatic conditions, i.e. the current was kept constant during the process and the anode potential was allowed to vary.

PEO-treated specimens were examined by a Philips XL30 scanning electron microscope (SEM) equipped with an energy-dispersive x-ray (EDS) attachment. Cross-sections were prepared by grinding through successive grades of SiC paper, with final polishing to a $0.1 \mu\text{m}$ diamond finish. A Mira3-XMU Field Emission SEM (FESEM) was employed to obtain high magnification images, elemental maps of the cross-sections, and study the surface morphology of coated samples. Samples were sputter coated with gold prior to SEM imaging to minimize surface charging. A Philips X’Pert_MRD diffractometer with $\text{Cu K}\alpha$ (40 kV and 30 mA) radiation was used to study the phase composition of coatings. Samples were scanned in the 2θ range from 30° to 70° with a 0.05° step size. The X’pert Highscore software with PDF2 database was employed to analyze XRD patterns.

3. Results and discussion

3.1. Voltage-time behavior

Plots showing potential variations of samples during the PEO process at a constant current density of 5 A dm^{-2} in electrolytes containing different concentrations of ZnO nanoparticles are presented in figure 1. Examining the voltage-time plots reveals up to three stages can be identified. In the first stage, voltage increases almost linearly within a short period to about 500 V with an average slope of 48 V s^{-1} . During this stage, the barrier oxide film grows at a constant rate (Stage I in figure 1) and the main part of the total current passing through the film is ionic current, which forms the oxide film [5]. As a result, the potential needs to increase in order to compensate for the increase of ionic resistance due to film growth [9]. At this stage, gas bubbles are formed on the surface of the substrate [11].

At 490 V , close to the region where a major reduction in the slope of the voltage-time response is observed in figure 1, the breakdown potential is reached and many small-sized micro-discharges with a white color appear over the entire surface of the sample [5, 20]. After the breakdown potential, anodization voltage still increases, but the voltage-time slope decreases towards a relatively constant value of anodization voltage (Stage II in figure 1). In stage III, the rate of voltage change increases more relative to stage II. Micro-discharges become more intense than before and their color changes from white to yellow and then gradually to orange. In addition some studies report, the MAO process was split into four stages and in last stage, sparks became even stronger, exerting a detrimental effect on the qualities of coating [20, 21].

Electrolytes with different contents of ZnO nanoparticles were opaque, which prevented the visual assessment of sparking behavior during the PEO process. However, the particle additions did not appear to significantly affect sparking, as evaluated from the shapes of the voltage-time response plots. This suggests that the addition of ZnO nanoparticles did not influence the electrolyte properties and deposition mechanism significantly. This observation was found to agree with previous studies in the literature [3, 5, 9].

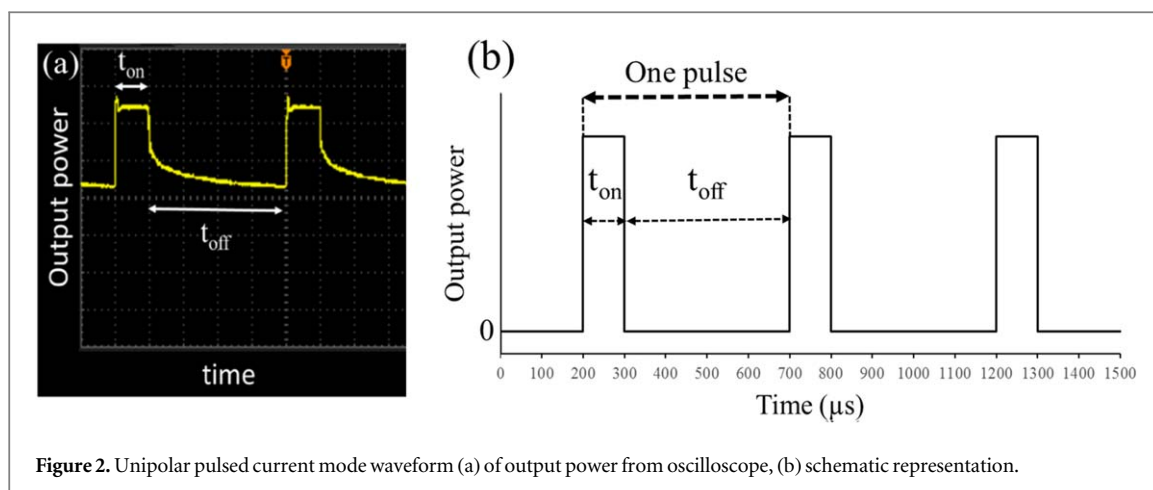
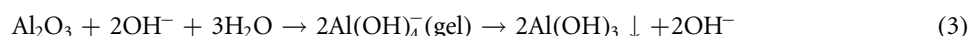
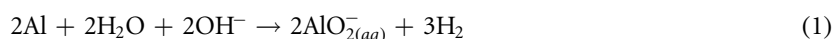


Figure 2. Unipolar pulsed current mode waveform (a) of output power from oscilloscope, (b) schematic representation.

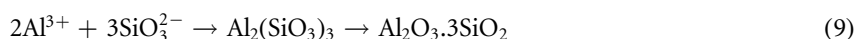
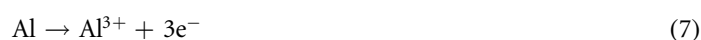
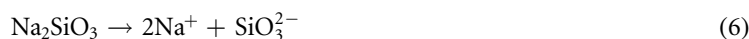
An oscilloscope was used to monitor and record the waveform during the coating process. A snapshot of the oscilloscope screen showing the waveform produced by the power supply and a schematic representation of the waveform at a duty cycle of 20% and a frequency of 2000Hz are illustrated in figures 2(a) and (b), respectively.

Different processes such as oxide formation, dissolution and gas evolution may occur during the PEO coating process on aluminum in alkaline solutions [22]. In figure 2, the period t_{off} is attributed to the time when no current is applied. During this period, chemical reactions can etch the aluminum substrate and subsequently release aluminum ions into the electrolyte through Reactions (1) [23] and (2) [22, 23]. In addition, the thickness of the alumina coating can decrease as a result of chemical dissolution, Reaction (3) [22, 23].



Based on the above reactions, during the t_{off} period, only the surface of Al substrate is chemically dissolved by reacting with OH^- , originating from KOH in the electrolyte, Reaction (5). Since the electrolyte is continuously agitated during the PEO process, there is no limitation for OH^- anions to diffuse to the electrode surface and chemical processes [22].

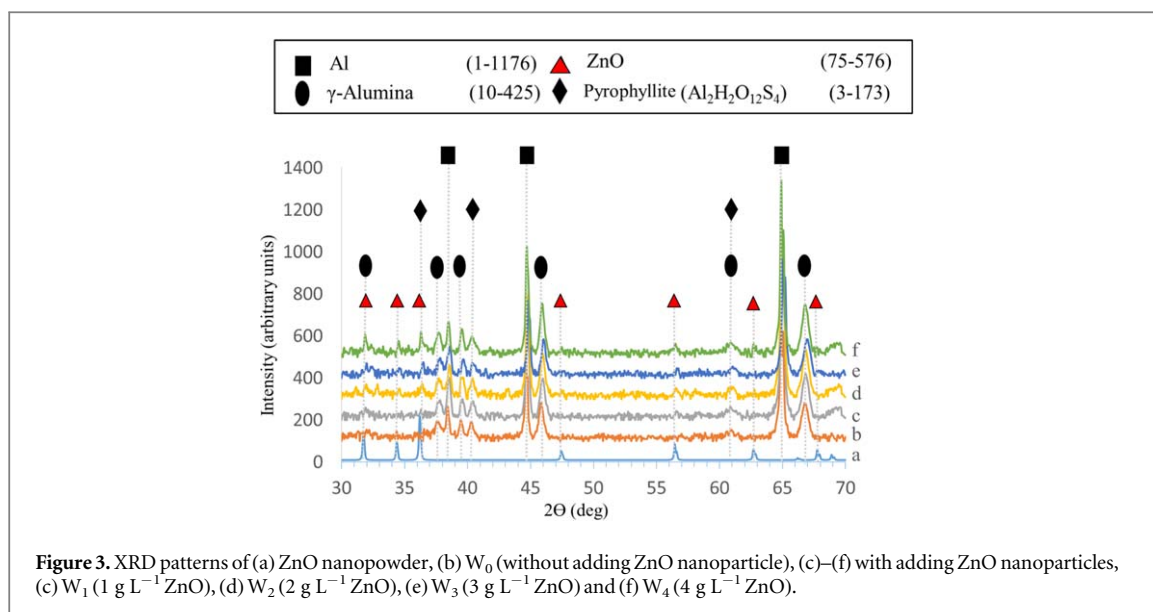
During the t_{on} period, figure 2, micro-discharges start to appear above the breakdown potential. Due to the high electric fields generated during the PEO process, the electrolyte components (potassium hydroxide, sodium silicate and water) can be ionized and decomposed according to the Reactions (4)–(6) [11]. Anodic dissolution of aluminum releases cations into the electrolyte, Reaction (7) [22]. Under the influence of the high electric field, oxygen anions (O^{2-}) diffuse towards the substrate. Finally, oxygen anions react with metal cations (Al^{3+}), migrating out across the former coating towards the electrolyte, to form aluminum oxide, Reaction (8) [22, 23]. Prior research suggests that some of the aluminum cations might be ejected into the electrolyte and react with silicate, resulting in the formation of mullite, Reaction (9) [12, 23].



Based on this set of reactions, it can be concluded that a combination of mainly alumina and some alumina-silicate phases is expected to form during the PEO process applied to aluminum substrates in alkali electrolytes containing sodium silicate [23].

3.2. Phase composition

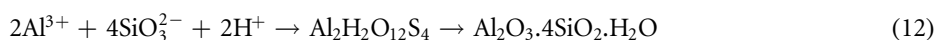
X-ray diffraction patterns of PEO coatings treated in electrolytes with different contents of ZnO nanoparticles are presented in figure 3. Inspection of the XRD spectra revealed that the coatings were mainly composed of γ - Al_2O_3 and $Al_2H_2O_{12}Si_4$ ($Al_2O_3 \cdot 4SiO_2 \cdot H_2O$). Aluminum peaks, originating from the substrates, are also observed. In addition to Al, γ - Al_2O_3 and $Al_2H_2O_{12}Si_4$, in samples prepared in electrolytes containing various amounts of nano-particles, figures 3(c)–(f) (W_1 – W_4), ZnO was also detected.



Previous studies on PEO coated aluminum alloys in alkali silicate-based electrolytes suggest that the coatings are mainly composed of α - Al_2O_3 [3, 8, 20], γ - Al_2O_3 [3, 8, 9, 20], mullite ($3\text{Al}_2\text{O}_3 \cdot 2\text{SiO}_2$) [9, 20], or a mixture of these phases. It has been suggested that the molten material formed during sparking solidifies as γ - Al_2O_3 rather than α - Al_2O_3 upon contact with the electrolyte. Extremely high cooling rates experienced during solidification and lower critical energy for nucleation facilitates the formation of γ - Al_2O_3 [24]. Since γ - Al_2O_3 is a metastable phase, it can transform into α - Al_2O_3 in the temperature range of 1050 to 1200 °C and as the temperature increases, this phase transformation occurs at a faster rate [5, 8, 24].

Generally the main parameter in PEO coatings, which determines the η - Al_2O_3 / δ - Al_2O_3 / α - Al_2O_3 ratio is the heating mode related to the micro-discharges characteristics, such as power and duration, in the course of coating formation and its cooling rate [25]. By controlling the electrical parameters such as current density, duty cycle and frequency, it would be possible to control the transformation rate of γ to α - Al_2O_3 phase. Applying higher current densities has been shown to increase the localized temperature of micro-discharges, leading to enhanced coating growth rate and higher relative contents of α - Al_2O_3 [24, 26]. Lower duty cycles were found to result in micro-discharges with lower intensities but higher spatial densities [20]. Furthermore, micro-discharges are interrupted during the pulse off-time (t_{off}) in pulsed-unipolar current mode, allowing the surface to cool down [24]. Therefore, decreasing the duty cycle or increasing frequency would create less heat in the coating, keeping the temperature below the critical temperature required for γ to α - Al_2O_3 phase transformation. The electrical parameters used in this work, i.e., a low current density and duty cycle of 5 A dm^{-2} and 20%, respectively, and a high frequency of 2000 Hz did not create enough heat necessary for γ to transform to α - Al_2O_3 , which is why α - Al_2O_3 was not detected in the XRD patterns of PEO coated samples in this research.

Mullite or other alumina-silicate phases can form in PEO coatings depending on the temperature of the process, Reaction (9) [23]. Mullite is formed at temperatures above 1000 °C depending on the process route employed, possibly by a nucleation and growth mechanism involving a reaction between Al_2O_3 and SiO_2 [24]. As discussed earlier, employing a higher current density and duty cycle would increase the localized temperature of discharges, thus favoring the formation of Mullite [24]. Mullite was not detected in the PEO coatings synthesized under conditions used in this work. Another possible reaction involved is that anions will be attracted toward the surface due to the anodic polarization and produce silica, alumina, and other compositions [23] (Reactions (10) and (11)). Pyrophyllite is a hydrous alumina-silicate phase formed in this research according to Reaction (12). Formation temperature of pyrophyllite is lower than Mullite and thermal treatment of pyrophyllite causes the conversion of Mullite at temperatures higher than 1000 °C [27, 28].



In XRD patterns of samples prepared in electrolytes containing various amounts of nanoparticles, figures 3(c)–(f) (W_1 – W_4), ZnO peaks are detected, indicating incorporation of ZnO nanoparticles into the

coating. As can be seen in figures 3(c) to (f), ZnO peaks become stronger in electrolytes with higher concentrations of nanoparticles.

Previous studies have shown the point of zero charge (pzc), at which nanoparticles exhibit zero net electrical charge, for ZnO nanoparticles (pH_{PZC}) is between the pH ranges of 8.7 to 9.5. As the pH shifts towards higher pH values, zeta potential becomes more negative and the surface of the particles becomes more negatively charged [18]. The electrolyte used in this work had a pH of 12. At this high pH, ZnO species have a high negative zeta potential in the electrolyte. Higher absolute values of zeta potentials are desirable in PEO electrolytes containing nanoparticles since particles are more stable and resist agglomeration and settling. The negative charge on the particles will enhance their movement in the electric field created by the potential difference during the PEO process due to the cataphoretic effect, and promotes the incorporation of particles into the coating on the sample which is positively charged.

Based on the XRD results, ZnO nanoparticles are incorporated into the coating at the coating surface and following transport to the inner coating regions along short-circuit paths created by breakdown events. Similar results have been reported for electrolytic oxidation of magnesium in electrolytes containing monoclinic zirconia in the literature [7].

According to literature by adding sodium tungstate to the electrolyte solution, the corrosion resistance and hardness of the coatings significantly improved due to the incorporation of tungsten [29], but no phase containing Na_2WO_4 species was detected in the XRD patterns.

3.3. Coating morphology

Surface morphologies of PEO coated samples are presented in the SEM micrographs in figures 4(a)-(e), corresponding to samples W_{0-4} , respectively. Generally, all coatings contain numerous pores and craters all over the surface. These features are typical of breakdown events [24, 30]. Two distinct regions are distinguishable on the surface of all samples: (i) a significant portion of the surface is occupied by craters; a volcano-like microstructure formed by individual micro-discharge events, and (ii) a fine nodular structure consisting of small particles [24, 30]. Besides, micron-sized silicon-rich particles are also present in all coated samples. Such particles are often found on the surface of PEO coated samples in silicate-based electrolytes [7].

Scanning electron microscope images of the coating surface formed in the presence of ZnO nanoparticles at electrolyte disclosed an extensive regular network of light regions corresponding to coating decorated by ZnO-rich particles. Inspection of the SEM micrographs in figure 4 shows there are fewer cracks and open pores on the surface of coatings synthesized in electrolytes with higher contents of ZnO nanoparticles, suggesting that these surface defects have been partially filled with ZnO nanoparticles. This is consistent with what has been found in a previous study [9].

The distribution of elements on the surface of PEO coatings in figure 4 were determined using EDS surface analyses and the results are presented in table 2. Coatings were primarily composed of Al, O, Si, and Zn. Comparison of EDS results revealed that the amount of Zn increased in samples synthesized in electrolytes with higher ZnO contents. The Al/Si intensity ratios for different coatings obtained from surface EDS analysis are greater than 1.5 in all coatings. Additionally, elemental maps from the surface of sample W_4 are shown in figure 5. It reveals higher surface concentration of Al and lower Si.

In an earlier study [24] it was reported that Al/Si intensity ratio increased with decreasing duty cycle. At lower duty cycles, achieved via applying a shorter t_{off} and/or a higher frequency, more discharges occur resulting in more Al participating in the discharge process and thus increasing aluminum content on the coating surface [19]. In addition, it can be seen from figure 5 that ZnO nanoparticles were uniformly dispersed all over the coatings surface.

The SEM micrographs of PEO coating cross-sections of samples W_{1-4} , figure 6, reveal some porosity and discharge channels within the coating.

Based on the literature, PEO coatings can be comprised of up to three layers. The first one is the 'barrier layer', a thin inner layer located adjacent to the substrate. The barrier layer has a major contribution to corrosion protection [31]. The next one is the 'functional layer' or 'intermediate layer', which constitutes about 70%–80% of the total coating thickness and provides the main thermo-mechanical and tribological functionality of the coating. The third layer, located on top of the functional layer, is mainly loose and porous [20, 31].

Cross-sectional micrographs in figure 6 show all coatings are mainly composed of two layers, the thin barrier and functional layers, while the third porous layer can be seen in some parts of the coatings. Optical micrograph of cross-section of W_0 and W_4 is shown in figure 7. Coating thickness measurements showed that all coatings have a thickness of about $9 \pm 3 \mu\text{m}$ and no significant change is observed when comparing the cross-sections of coated samples in different electrolytes. In other words, the presence of ZnO nanoparticles did not influence the coating thickness during the PEO process.

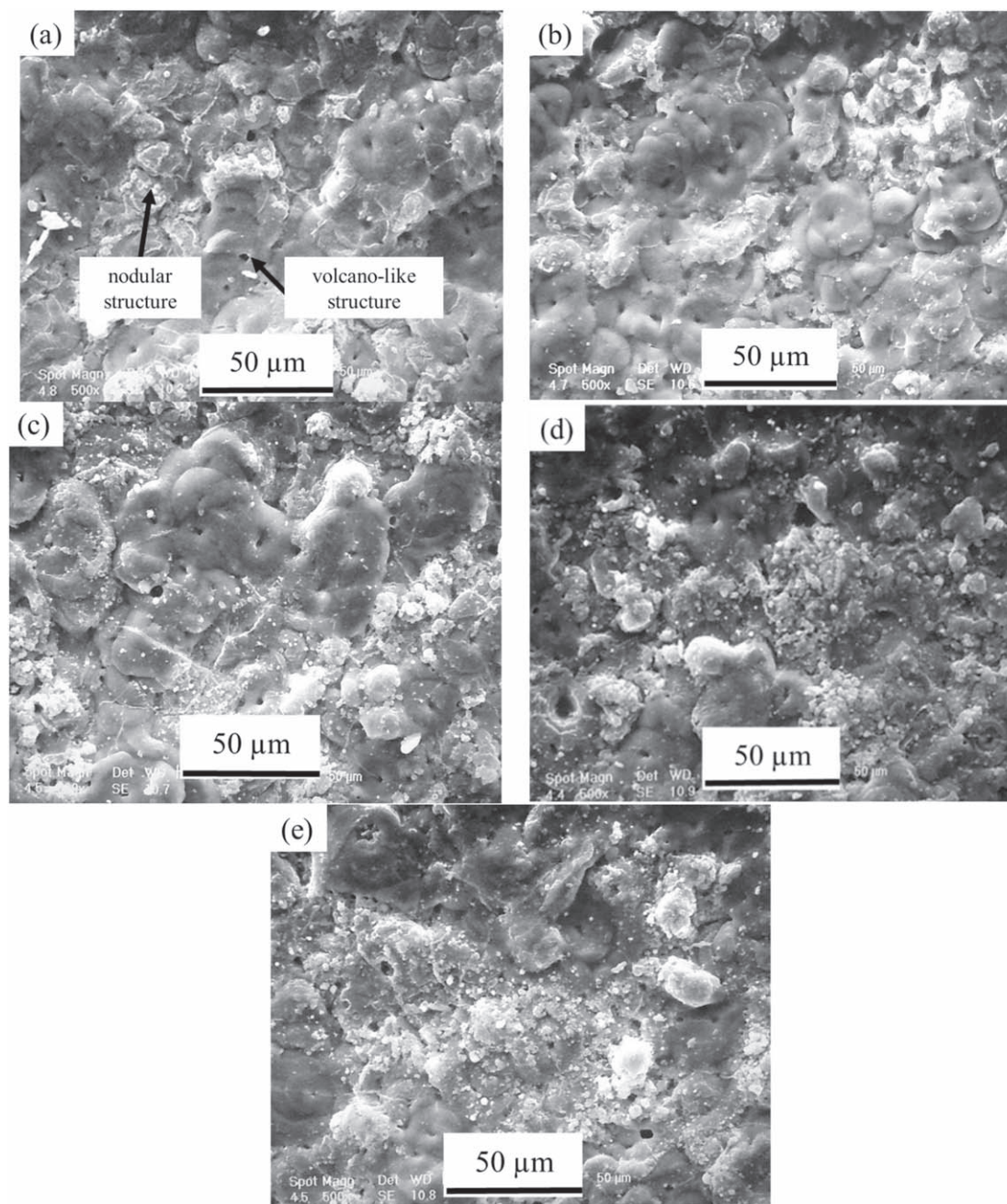


Figure 4. Surface morphology of PEO coatings without ZnO nanoparticles (a) W_0 , and with the addition of nanoparticles (b) W_1 (1 g L^{-1} ZnO), (c) W_2 (2 g L^{-1} ZnO), (d) W_3 (3 g L^{-1} ZnO) and (e) W_4 (4 g L^{-1} ZnO).

Table 2. Chemical composition of oxide coatings in figure 4 by EDS.

Sample	ZnO (g L^{-1})	Element (Wt%)			
		Al	O	Si	Zn
W_0	0	36.78	44.37	18.85	—
W_1	1	32.87	44.48	18.5	4.15
W_2	2	28.13	47.69	18.52	5.66
W_3	3	33.17	41.91	15.40	9.52
W_4	4	26.92	46.39	16.26	10.43

EDS elemental maps of mechanically polished cross-sections of sample W_4 revealed that Zn and Si were primarily concentrated in the upper parts of the coatings as well as near the coating-substrate interface (figure 8). In previous studies on PEO composite coatings synthesized in silicate-based electrolytes [3, 9] it was observed

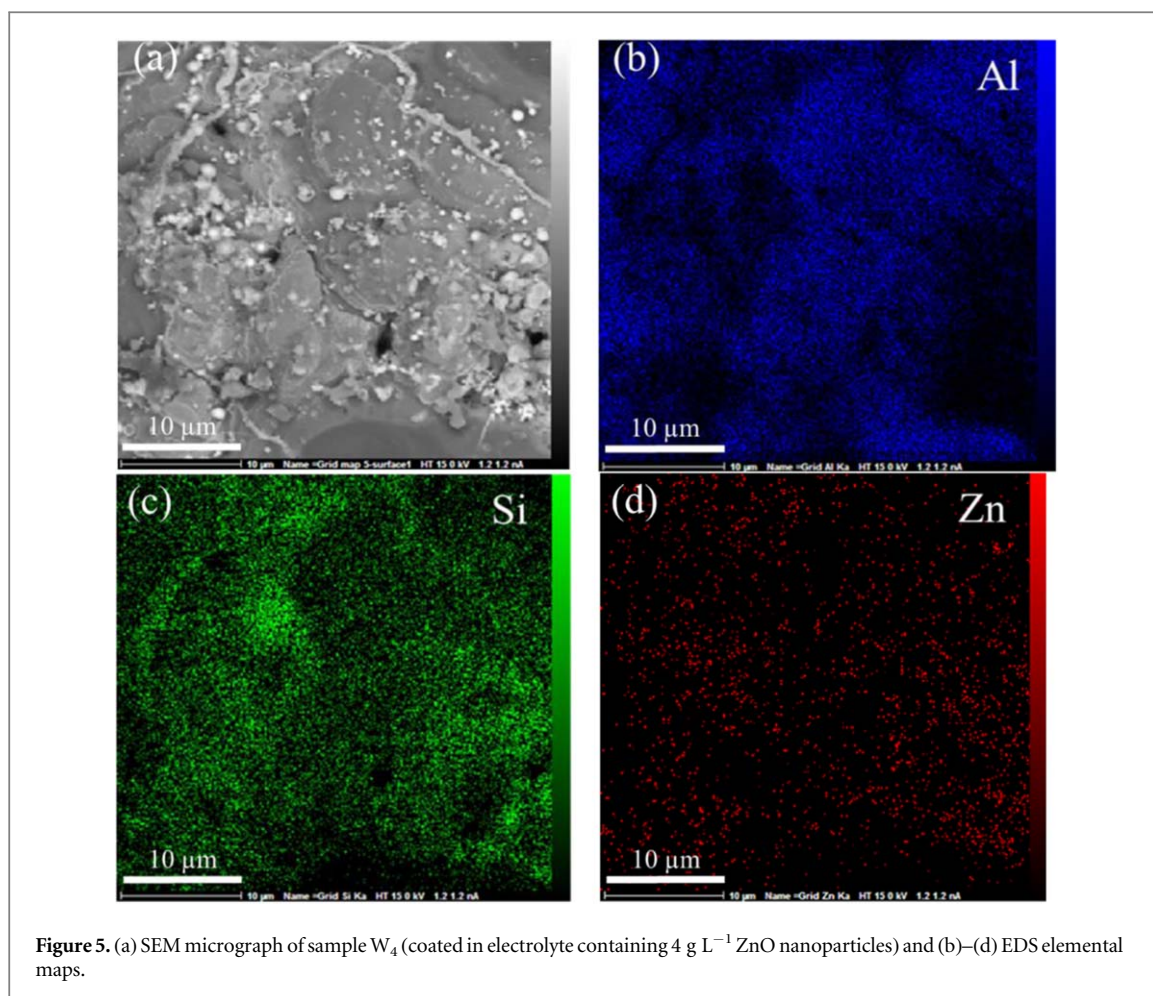


Figure 5. (a) SEM micrograph of sample W_4 (coated in electrolyte containing 4 g L^{-1} ZnO nanoparticles) and (b)–(d) EDS elemental maps.

that Si and added particles were mostly concentrated in the upper parts of the coatings, although a small number of particles could reach the inner parts through short-circuit paths. In another study [5] where boric acid and borax solutions were used to grow PEO coatings on aluminum, ZnO nanoparticles were found to be mainly located on the upper parts of the coatings, as well. In all the above mentioned studies, [3, 5, 9], DC mode was used. In PEO composite coatings prepared under AC mode, [7, 11, 32], a more uniform distribution of nanoparticles across the coatings has been reported. The applied current regime (DC, AC, pulsed-unipolar, or pulsed-bipolar) can affect surface discharge characteristics, namely the intensity and density of micro-discharges, which play a crucial role in determining coating properties [12]. The use of AC and/or pulsed DC mode would make it possible to control micro-discharge events by means of arc interruption and prevents overheating and destruction of coating that may occur under DC regimes [31]. However, invariable and fixed duty cycle (=50%) of AC mode is disadvantageous and restricts the commercial upscaling of this mode [12].

Employing pulsed DC mode makes it possible to control discharge duration by varying the duty cycle. A pulsed-bipolar current mode is comprised of three distinct periods consisting of (t_{on}^+), (t_{off}) and (t_{on}^-) corresponding to anodic current on-time, off-time, and cathodic current on-time, respectively. During (t_{on}^-) period, corresponding to the negative segment in AC current mode, cation species are attracted to the negatively charged substrate and anion species are repelled into the electrolyte [12]. Therefore, in spite of the high physical and mechanical characteristics of coatings are formed in electrolytes with high pH in AC or pulsed-bipolar current modes, employing these current modes to fabricate PEO composite coatings in electrolytes containing nanoparticle may negatively affect the incorporation of nanoparticles into the coating, since at high pH values of electrolytes typically used for PEO, particles have a negative surface charge (zeta potential). Pulsed-unipolar current mode, on the other hand, is comprised of an off-time (t_{off}) and a positive component (t_{on}^+), during which negatively charged particles are attracted towards the sample and seems to be more appropriate for incorporating particles into PEO composite coatings.

The high concentration of Si on the surface of the coatings in this research could be linked to micro-discharge behavior during PEO. It has been proposed that Si forms insoluble gels which reduce Si ionic mobility and as a result, a silicon-rich outer part is formed on the coating surface. Anion species or entrapped particles with high negative zeta potentials can also be found in this silica gel on the coating surface. Silicon and anion

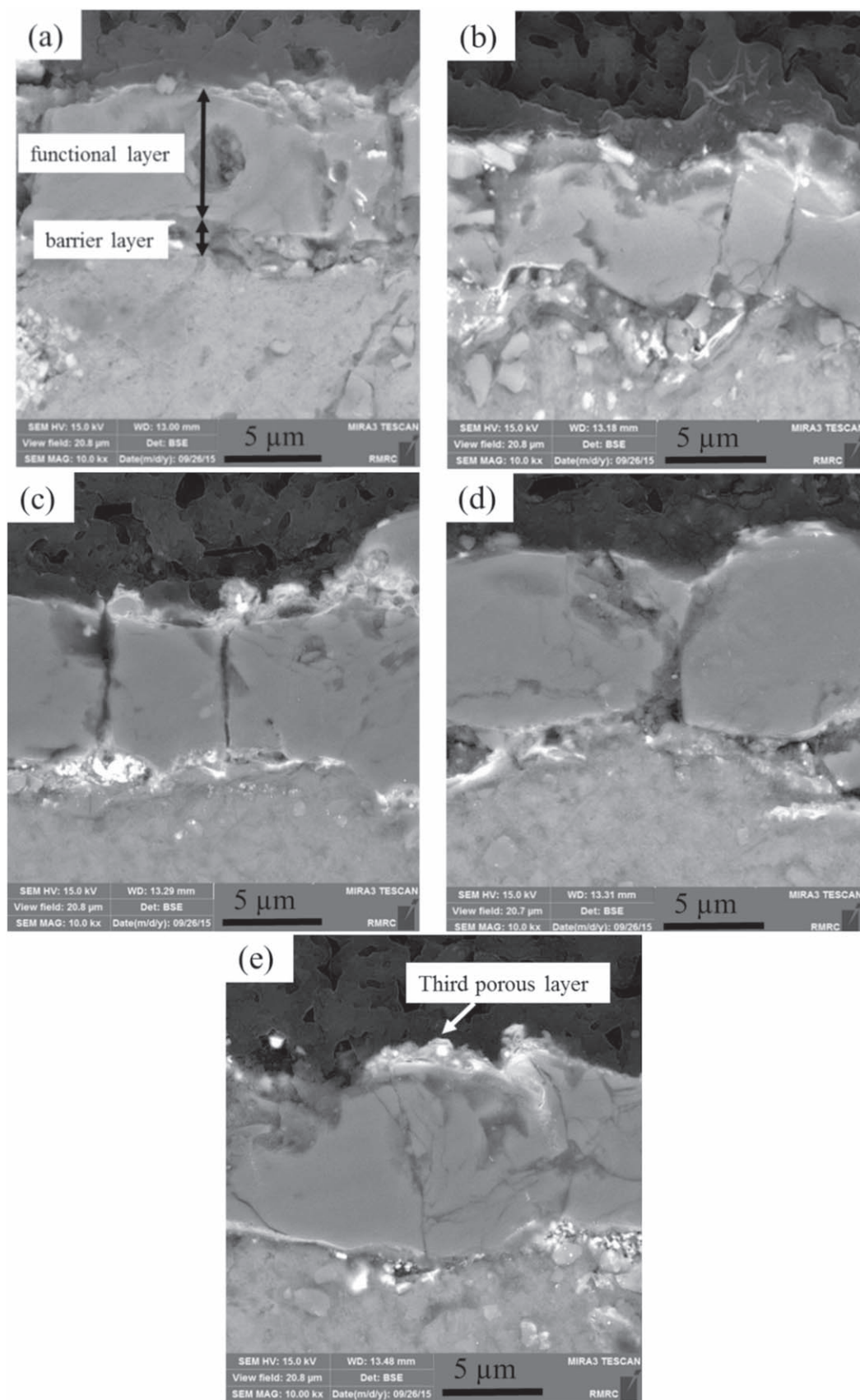


Figure 6. Cross-section images of (a) W_0 (without adding ZnO nanoparticle), (b)–(e) with adding ZnO nanoparticles, (b) W_1 (1 g L⁻¹ ZnO), (c) W_2 (2 g L⁻¹ ZnO), (d) W_3 (3 g L⁻¹ ZnO) and (e) W_4 (4 g L⁻¹ ZnO).

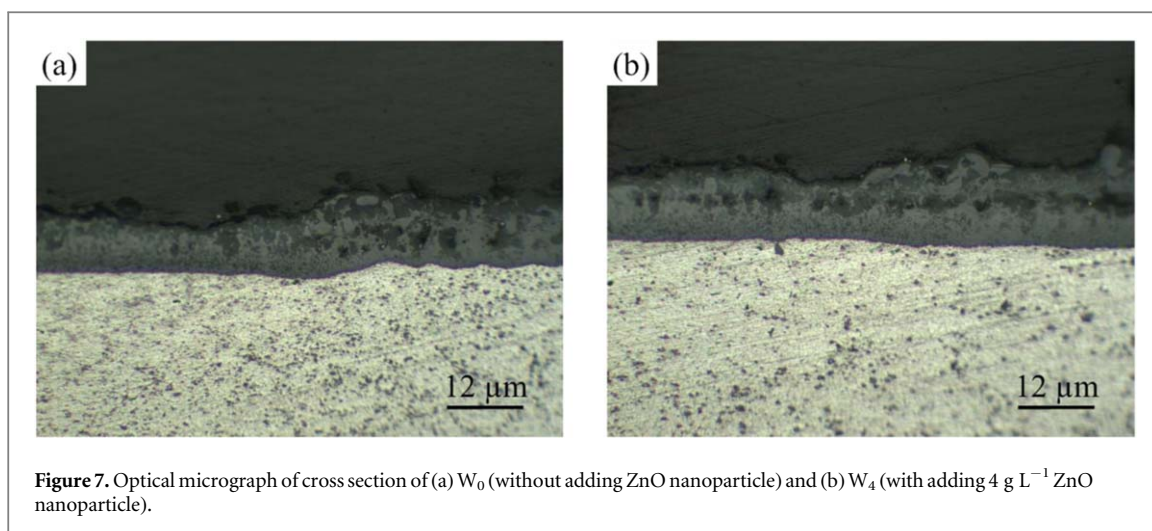


Figure 7. Optical micrograph of cross section of (a) W_0 (without adding ZnO nanoparticle) and (b) W_4 (with adding 4 g L⁻¹ ZnO nanoparticle).

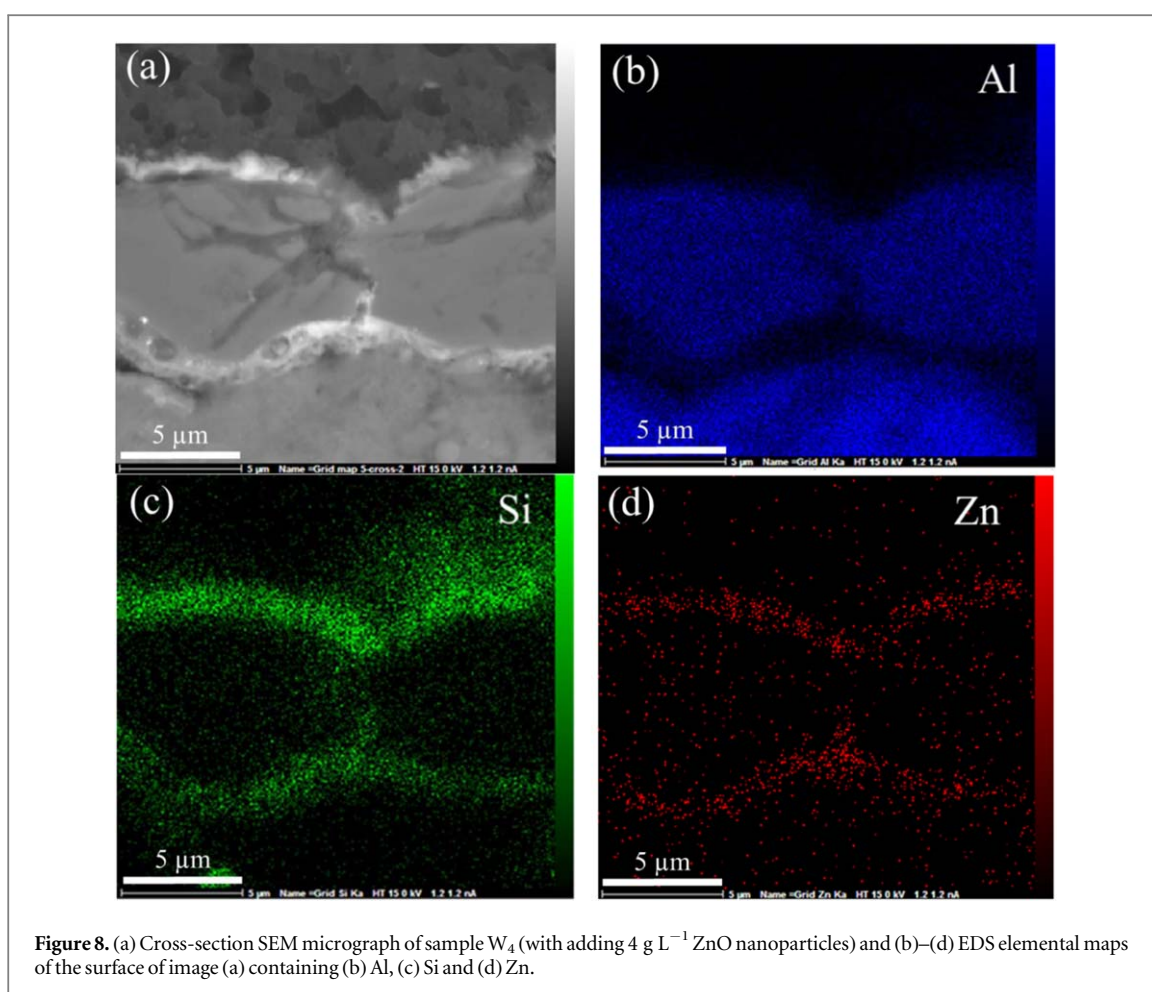
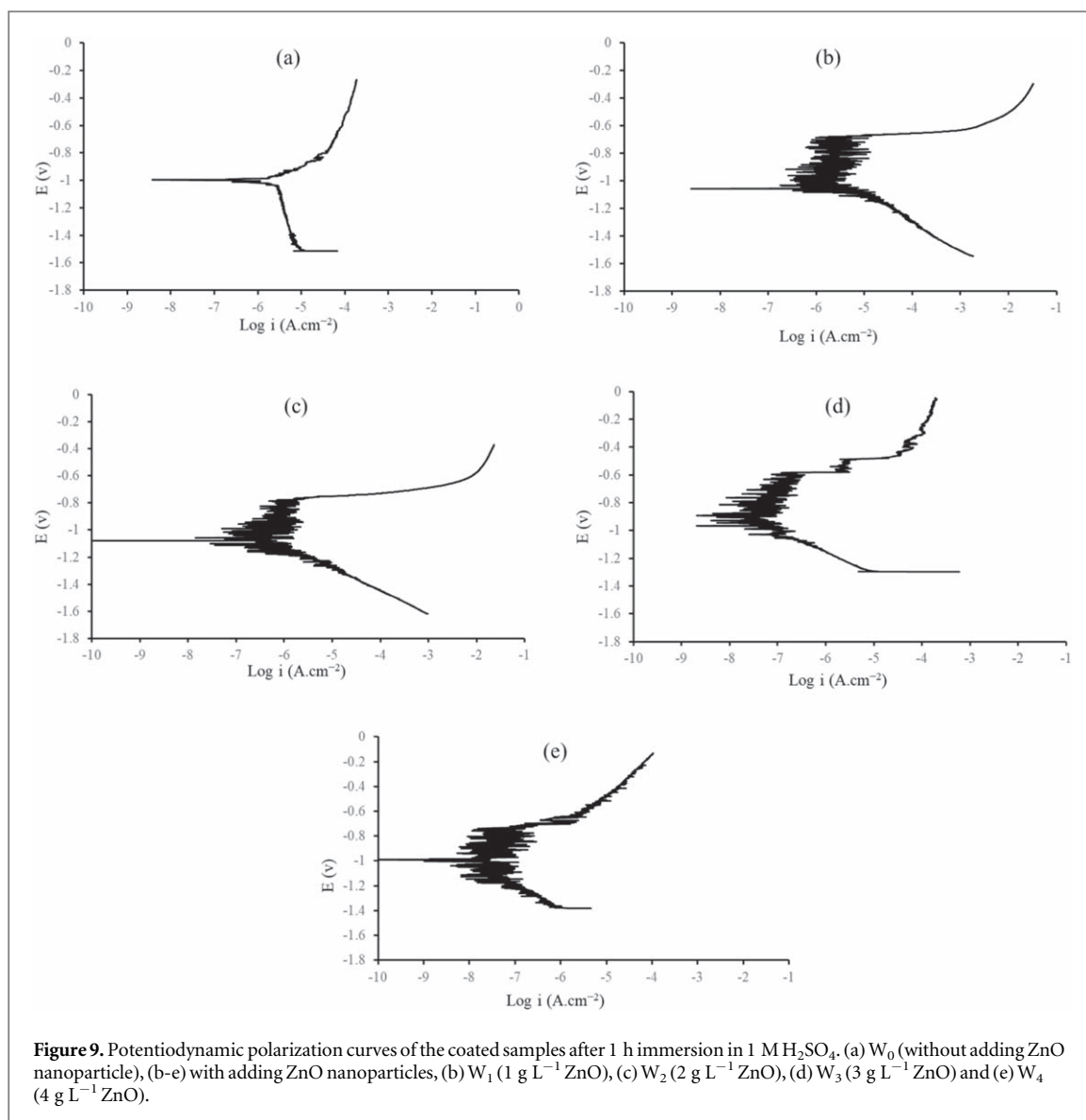


Figure 8. (a) Cross-section SEM micrograph of sample W_4 (with adding 4 g L⁻¹ ZnO nanoparticles) and (b)–(d) EDS elemental maps of the surface of image (a) containing (b) Al, (c) Si and (d) Zn.

species could be present in the alumina-rich region only due to short-circuit paths formed in breakdown events [3, 30].

At low duty cycles, micro-discharges are less intense, and their spatial density is higher due to the higher number of sparks on the surface. The applied current is distributed among all micro-discharge events during PEO. When there is a higher number of micro-discharge events present, a lower current passes through each individual micro-discharge channel [24]. Each micro-discharge ejects molten material onto the surface. The outward force caused by these ejections can detach adsorbed species such as silicon, SiO_3^{2-} , or ZnO nanoparticles from the surface. Therefore, when a low duty cycle is applied during the PEO process, the corresponding large number of micro-discharges created will remove most of the negatively charged adsorbed species from the surface during the on-time. During cooling of a solidified crater at a discharge site, anion species



in the electrolyte can enter discharge channels under a strong electric field through electrophoresis and reach the inner parts of the coating [12]. This could explain why Si and Zn elements were distributed on top of the coating, as well as in a narrow band between the coating and the substrate, figure 8 part c and d.

Furthermore, based on experimental results, an aggregation of ZnO particles near the coating-substrate interface has been observed. It seems that there is a different mechanism for ZnO incorporation into the oxide coating in the early and later stages of PEO. In the early stages of PEO treatment, ZnO particles quickly accumulate on the surface of the substrate due to the strong electric fields formed and the high negative zeta potential of particles. Then, a thin layer of PEO coating is formed and further accessibility of particles to the substrate surface is lost. Afterwards, particles can only reach the inner layer of the coating through short-circuit paths formed by breakdown events. Finally, in the later stages of PEO, particle concentration increases at the coating surface through deposition of silica gel containing entrapped ZnO particles.

3.4. Corrosion behavior

Potentiodynamic polarization test were employed to investigate the corrosion behavior of the samples in 1 M H₂SO₄ medium. The results are depicted in figure 9 and corrosion potential (E_{corr}) and corrosion current density (I_{corr}) were derived directly from the polarization curves and showed at table 3. Although there was no major change in values of E_{corr} for compared samples, the values for I_{corr} do show a significant change. The I_{corr} value for the W₄ sample ($I_{\text{corr}} = 2.2 \times 10^{-8}$ A.cm⁻²) is two orders of magnitude higher than that for the W₀ sample ($I_{\text{corr}} = 2.8 \times 10^{-6}$ A.cm⁻²). The coatings porosity is known as the most important defect of PEO coatings, i.e., in the case of corrosion, they can decrease the protection ability by letting the corrosive media to penetrate through the coating [10, 11, 33]. As in the previous sections has been mentioned, the presence of ZnO

Table 3. Potentiodynamic polarization curve analysis results.

Sample	ZnO (g L ⁻¹)	I _{corr} (A.cm ⁻²)	E _{corr} (V)
W ₀	0	2.8 × 10 ⁻⁶	-0.99
W ₁	1	2.2 × 10 ⁻⁶	-1.06
W ₂	2	5.6 × 10 ⁻⁷	-1.05
W ₃	3	5.1 × 10 ⁻⁸	-0.96
W ₄	4	2.2 × 10 ⁻⁸	-0.99

nanoparticles did not influence the coating thickness during the PEO process, but there are fewer cracks and open pores on the surface of coatings with higher contents of ZnO nanoparticles. Therefore with decreasing the content of nanoparticles embedded in the coating structure corrosive ions could transfer more easily from surface to substrate, due to its higher porosity and corrosion resistance decreased. The coating of W₄ having highest ZnO nanoparticles has the lowest corrosion current density. As a results it must be mentioned that the addition of ZnO in the PEO coating leads to increased corrosion resistance.

4. Conclusion

The formation plasma electrolytic oxidation Al₂O₃ oxide composite coatings containing ZnO nanoparticles was investigated in this work. Samples were coated in a silicate-based electrolyte under pulsed-unipolar current mode. Applying pulsed DC current allows the control of discharge duration by means of changing the duty cycle. Applying lower duty cycles resulted in microdischarges with a higher spatial density and a lower intensity. A shorter duty cycle and a lower current density would decrease the localized temperature of the discharges, therefore, lowering the probability of α -Al₂O₃ and mullite formation. γ -Al₂O₃ and Pyrophyllite are the main phases formed in the coating in this research under a low duty cycle of 20% and a current density of 5 A dm⁻².

Additionally experimental results revealed that Zn and Si were primarily concentrated in the upper parts of the coatings as well as near the coating-substrate interface. It has been proposed that Si forms insoluble gels which reduce Si ionic mobility and as a result, a silicon-rich outer part is formed on the coating surface. Anion species or entrapped particles with high negative zeta potentials can also be found in this silica gel on the coating surface, which is why ZnO nanoparticles were primarily distributed in the upper parts of the coatings. Also in pulsed-unipolar DC current mode with a low duty cycle, the corresponding large number of micro-discharges created will remove most of the negatively charged adsorbed species from the surface during the on-time. Then during cooling of a solidified crater at a discharge site, anion species in the electrolyte can enter discharge channels under a strong electric field through electrophoresis and reach the inner parts of the coating. Finally corrosion behavior of coatings investigated by potentiodynamic polarization test and results revealed that composite coatings with higher content of ZnO nanoparticles had better corrosion resistance.

Funding

This study was funded by the Iran National Science Foundation under grant agreement no. 96000484.

Authors' contributions

S Shahzamani, A Ashrafi and M Toroghinejad planned the experiments, analyzed and interpret the results. S Shahzamani and A Hakimizad contributed to sample preparation and performed the experiments. S Shahzamani wrote the manuscript. A Ashrafi, M Toroghinejad and V Dehnavi revised the manuscript. All authors provided critical feedback on the research, analysis and manuscript.

Conflict of Interest

Prof M Toroghinejad has received research grants from the Iran National Science Foundation.

ORCID iDs

Safoora Shahzamani  <https://orcid.org/0000-0002-2692-1196>

Ali Ashrafi  <https://orcid.org/0000-0001-5393-5860>

References

- [1] Wirtz G P, Brown S D and Kriven W M 1991 Ceramic coatings by anodic spark deposition *Mater. Manuf. Process.* **6** 87–115
- [2] Martin J, Melhem A, Shchedrina I, Duchanoy T, Nominé A, Henrion G, Czerwicz T and Belmonte T 2013 Effects of electrical parameters on plasma electrolytic oxidation of aluminium *Surface & Coatings Technology* **221** 70–6
- [3] Matykina E, Arrabal R, Monfort F, Skeldon P and Thompson G E 2008 Incorporation of zirconia into coatings formed by DC plasma electrolytic oxidation of aluminium in nanoparticle suspensions *Appl. Surf. Sci.* **255** 2830–9
- [4] James A 2005 Thermal and mechanical properties of plasma electrolytic oxide coatings *PhD dissertation* University of Cambridge
- [5] Stojadinović S, Tadić N, Radić N, Stojadinović B, Grbić B and Vasilčić R 2015 Synthesis and characterization of Al₂O₃/ZnO coatings formed by plasma electrolytic oxidation *Surface & Coatings Technology* **276** 573–9
- [6] Rožić L J, Petrović S, Radić N, Stojadinović S, Vasilčić R, Stefanov P and Grbić B 2013 Fractal approach to surface roughness of TiO₂/WO₃ coatings formed by plasma electrolytic oxidation process *Thin Solid Films* **539** 112–6
- [7] Arrabal R, Matykina E, Viejo F, Skeldon P, Thompson G E and Merino M C 2008 AC plasma electrolytic oxidation of magnesium with zirconia nanoparticles *Appl. Surf. Sci.* **254** 6937–42
- [8] Shoaie-Rad V, Bayati M R, Zargar H R, Javadpour J and Golestani-Fard F 2012 *In situ* growth of ZrO₂–Al₂O₃ nano-crystalline ceramic coatings via micro arc oxidation of aluminum substrates *Mater. Res. Bull.* **47** 1494–9
- [9] Bahramian A, Raeissi K and Hakimzad A 2015 An investigation of the characteristics of Al₂O₃/TiO₂ PEO nanocomposite coating *Appl. Surf. Sci.* **351** 13–26
- [10] White L, Koo Y, Yun Y and Sankar J 2013 TiO₂ deposition on AZ31 magnesium alloy using plasma electrolytic oxidation *Journal of Nanomaterials* **2013** 11–9
- [11] Sarbishei S, Faghihi Sani M A and Mohammadi M R 2014 Study plasma electrolytic oxidation process and characterization of coatings formed in an alumina nanoparticle suspension *Vacuum* **108** 12–9
- [12] Dehnavi V 2014 Surface modification of aluminum alloys by plasma electrolytic oxidation *PhD dissertation* University of Western Ontario
- [13] Liu Y, Xu J, Gao Y, Yuan Y and Gao C 2012 Influences of additive on the formation and corrosion resistance of micro-arc oxidation ceramic coatings on aluminum alloy *Physics Procedia* **32** 107–12
- [14] Bouhamed H and Baklouti S 2014 Synthesis and characterization of Al₂O₃/ZnO nanocomposite by pressureless sintering *Powder Technol.* **264** 278–90
- [15] Sun Y H, Xiong W H and Li C H 2010 Fabrication of ultrahigh density ZnO–Al₂O₃ ceramic composites by slip casting *Transactions of Nonferrous Metals Society of China* **20** 624–31
- [16] Hanaor et al 2012 The effects of carboxylic acids on the aqueous dispersion and electrophoretic deposition of ZrO₂ *J. Eur. Ceram. Soc.* **32** 235–44
- [17] Marsalek R 2014 Particle size and zeta potential of ZnO *APCBEE Procedia* **9** 13–7
- [18] Fatehah M O, Aziz H A and Stoll S 2014 Stability of ZnO nanoparticles in solution. Influence of pH, dissolution, aggregation and disaggregation effects *Journal of Colloid Science and Biotechnology* **3** 75–84
- [19] Dehnavi V, Luan B L, Shoesmith D W, Liu X Y and Rohani S 2013 Effect of duty cycle and applied current frequency on plasma electrolytic oxidation (PEO) coating growth behavior *Surf. Coat. Technol.* **226** 100–7
- [20] Dehnavi V, Luan B L, Liu X Y, Shoesmith D W and Rohani S 2015 Correlation between plasma electrolytic oxidation treatment stages and coating microstructure on aluminum under unipolar pulsed DC mode *Surf. Coat. Technol.* **269** 91–9
- [21] Gu X, Jiang B, Li H, Liu C and Shao L 2018 Properties of micro-arc oxidation coatings on aluminum alloy at different negative peak current densities *Mater. Res. Express* **5** 056522
- [22] Snizhko L O, Yerokhin A L, Pilkington A, Gurevina N L, Misnyankin D O, Leyland A and Matthews A 2004 Anodic processes in plasma electrolytic oxidation of aluminium in alkaline solutions *Electrochim. Acta* **49** 2085–95
- [23] Al Bosta M M, Ma K J and Chien H H 2013 The effect of MAO processing time on surface properties and low temperature infrared emissivity of ceramic coating on aluminium 6061 alloy *Infrared Phys. Technol.* **60** 323–34
- [24] Dehnavi V, Liu X Y, Luan B L, Shoesmith D W and Rohani S 2014 Phase transformation in plasma electrolytic oxidation coatings on 6061 aluminum alloy *Surf. Coat. Technol.* **251** 106–14
- [25] Terleeva O P, Slonova A and Belevantsev V I 2018 Strength characteristics of 2024 aluminum alloy substrate with plasma electrolytic oxidation coatings *Mater. Res. Express* **5** 096508
- [26] Dou Q, Li W, Zhang G, Zhu W and Zhou Y 2018 Effects of anodic and cathodic current densities on microstructure, phase composition and properties of plasma electrolytic oxidation ceramic coatings on 6063 aluminum alloy *Mater. Res. Express* **5** 116407
- [27] Sanchez-Soto P J and Perez-Rodriguez J L 1989 Formation of mullite from pyrophyllite by mechanical and thermal treatments *J. Am. Ceram. Soc.* **72** 154–7
- [28] Heller L 1962 The thermal transformation of pyrophyllite to mullite *American Mineralogist* **47** 156–57
- [29] Hakimzad A, Raeissi K, Santamari M and Asgharia M 2018 Effects of pulse current mode on plasma electrolytic oxidation of 7075 Al in Na₂WO₄ containing solution: from unipolar to soft-sparking regime *Electrochim. Acta* **284** 618–29
- [30] Monfort F, Berkani A, Matykina E, Skeldon P, Thompson G E, Habazaki H and Shimizu K 2007 Development of anodic coatings on aluminium under sparking conditions in silicate electrolyte *Corros. Sci.* **49** 672–93
- [31] Matykina E, Arrabal R, Skeldon P and Thompson G E 2009 Investigation of the growth processes of coatings formed by AC plasma electrolytic oxidation of aluminium *Electrochim. Acta* **54** 6767–78
- [32] Mohedano M, Blawert C and Zheludkevich M L 2015 Silicate-based plasma electrolytic oxidation (PEO) coatings with incorporated CeO₂ particles on AM50 magnesium alloy *Mater. Des.* **86** 735–44
- [33] Curran J A and Clyne T W 2006 Porosity in plasma electrolytic oxide coatings *Acta Mater.* **54** 1985–93